



HAL
open science

Meso-Ester Corroles

Gabriel Canard, Di Gao, Anthony d'Aléo, Michel Giorgi, Florian-Xuan Dang,
Teodor Silviu Balaban

► **To cite this version:**

Gabriel Canard, Di Gao, Anthony d'Aléo, Michel Giorgi, Florian-Xuan Dang, et al.. Meso-Ester Corroles. Chemistry - A European Journal, In press. hal-01783843

HAL Id: hal-01783843

<https://amu.hal.science/hal-01783843v1>

Submitted on 4 May 2018

HAL is a multi-disciplinary open access archive for the deposit and dissemination of scientific research documents, whether they are published or not. The documents may come from teaching and research institutions in France or abroad, or from public or private research centers.

L'archive ouverte pluridisciplinaire **HAL**, est destinée au dépôt et à la diffusion de documents scientifiques de niveau recherche, publiés ou non, émanant des établissements d'enseignement et de recherche français ou étrangers, des laboratoires publics ou privés.

Meso-Ester Corroles

Gabriel Canard,^{*[a]} Di Gao,^[b] Anthony D'Aléo,^[a] Michel Giorgi,^[c] Florian-Xuan Dang,^[b] and Teodor Silviu Balaban^{*[b]}

Dedicated to Professor Mieczysław Józef Mąkosza on the occasion of his 80th birthday.

Abstract: The introduction of ester groups on the 5 and 15 *meso* positions of corroles stabilizes them against oxidation and induces a red-shift of their absorption and emission spectra. These effects are studied through the photophysical and electrochemical characterization of up to sixteen different 5,15-diester corroles where the third *meso* position is free or occupied by an aryl group, a long alkyl chains or an ester moiety. The single crystal X-ray structure analysis of five 5,15-diester-corroles and Density Functional Theory (DFT) and Time Dependent Density Functional Theory (TD-DFT) calculations, show that the strong electron withdrawing character of the 5,15 ester substituents is reinforced by their π -overlapping with the macrocycle aromatic system. The crystal packings of corroles **2**, **4**, **6**, **9** and **15** feature short distances between chromophores that are stacked into columns thanks to the low steric hindrance of *meso* ester groups. This close packing is partially due to intermolecular interactions involving inner hydrogen and nitrogen atoms and thereby stabilizing a single and identical corrole tautomeric form.

Introduction

In 1964, Johnson and Kay described the first synthesis of a corrole in which one *meso* carbon atom of the porphyrin skeleton is replaced by a direct pyrrole-pyrrole bond that implies the presence of three inner hydrogen atoms.^[1] The first synthetic accesses to corroles were essentially based on the cyclisation of *a,c*-biladienes which requires the time consuming preparation of β -substituted pyrrole and dipyrromethane units.^[2] For this reason, the reactivity and properties of corroles and their metal complexes were rather unexplored during more than thirty years.

In 1994 and 1996, the formation of corrole traces during the syntheses of symmetrical *meso*-tetraarylporphyrins proved that a simple one-pot pyrrole-aldehyde condensation could be used to prepare *meso*-triarylcorroles.^[3] This straightforward procedure was applied when the first one-pot preparations of *meso*-triarylcorroles were described in 1999.^[4] It was shown latter, that the corrole's precursor is an open chain tetrapyrrolic oligomer named bilane which is oxidized into corrole.^[5] Different strategies are now available to prepare *in situ* symmetrical and

unsymmetrical bilanes that are oxidized into simple to very sophisticated corroles with yields up to 60% or alternatively condensed with another aldehyde to give A_3B_2 -, *trans*- A_2B_2 - or AB_2C porphyrins.^[6] Consequently, corroles are now receiving an increased attention mainly because of two interesting features. The first one is their ability to stabilize metal ions in high oxidation states such as Fe^{IV} ,^[7] Au^{III} ,^[8] Th^{IV} ,^[9] or recently Pt^{IV} ,^[10] that led to the application of the remarkable metallocorroles properties in the fields of catalysis,^[11] sensors^[12] or medicine.^[13] The second important corroles feature is the high luminescence quantum yields of their free bases^[14] which has been used in imaging,^[13a,15] singlet oxygen sensitization^[14c,16] or to build sensors^[17] and photoactive arrays.^[18]

However, the increasing use of corrole free bases in applied research area suffers from their moderate stability towards oxidants. They may react with light, oxygen or quinones to produce open chain tetrapyrroles,^[14a,19] porphyrins,^[20] β - β' coupled oligomers^[21] or isocorroles.^[22] The fragility of free base derivatives is also illustrated by several examples of corrole's ring expansion.^[23] The stabilization of corroles against oxidation requires *meso* electron withdrawing substituents such as pentafluorophenyl groups. Consequently, elaborate corrole based structures are usually build on the derivatization of *meso* aryl groups or through the functionalization of β positions which often leads to complex mixtures of isomers. On the other hand, the preparation of corroles assemblies producing efficient energy and/or charge transport properties requires a good intermacrocycle overlapping which is hardly compatible with the steric hindrance of multiple *meso* aryl groups.

We describe here how the introduction of *meso* ester groups on the 5 and 15 *meso* positions of corroles is a good alternative to bulky aryl groups in order to stabilize corroles against oxidation. The influence of these groups on the corrole physico-chemical properties is studied by the photophysical and electrochemical characterization of up to sixteen different 5,15-diester corroles where the remaining *meso* position is occupied by i) an electron withdrawing aryl group or ii) an electron donating aryl group or iii) a long alkyl chains or iv) an ester group or v) a hydrogen atom. Density Functional Theory (DFT) and Time Dependent Density Functional Theory (TD-DFT) calculations, supported by single crystal X-ray structure analyses, show that the strong electron withdrawing character of the 5,15 ester substituents is reinforced by their π -overlapping with the macrocycle aromatic system. This π -conjugation is due to the low steric hindrance of ester groups which is put into evidence in five different crystal structures where the chromophores are stacked into columns featuring short intermacrocycle distances. The close packing of the chromophores is partially due to intermolecular interactions involving inner hydrogen and nitrogen atoms and thereby stabilizing a single and identical tautomeric form of the macrocycle.

[a] Dr. A. D'Aléo, Dr. G. Canard
Aix Marseille Université, CNRS UMR 7325
Centre Interdisciplinaire de Nanosciences de Marseille (CINaM)
13288 Marseille, France
Fax: (+33) 491 41 8916
E-mail: gabriel.canard@univ-amu.fr
Homepage: <http://www.cinam.univ-mrs.fr>

[b] Dr. D. Gao, F.-X. Dang, Prof. Dr. T. S. Balaban
Aix Marseille Université, Centrale Marseille, CNRS UMR 7313
Institut des Sciences Moléculaires de Marseille (ISM2),
Chirosciences
13397 Marseille Cedex 20, France
E-mail: ts.balaban@univ-amu.fr
Homepage: <http://ism2.univ-amu.fr>

[c] Dr. M. Giorgi
Fédération des Sciences Chimiques de Marseille – Spectropole FR
1739
Aix Marseille Université
13397, Marseille, France

Results and Discussion


Synthesis and characterization

Recently, Gust *et al.* described the synthesis of the 5,10,15,20-tetra(ethoxycarbonyl)porphyrin starting from the 5-(ethoxycarbonyl)dipyrromethane (EDPM) (Scheme 1).^[24] This result prompted us to employ the latter compound as a precursor of 5,15-di(ethoxycarbonyl)corrole derivatives (Scheme 1). Various described synthetic procedures were investigated. Our yields, although still in the single digit region, were obtained using the experimental conditions of a refined synthesis of trans-A₂B corroles published by Gryko *et al.* in 2004.^[6g] A key factor of this procedure is the addition of a quite high amount of trifluoroacetic acid (TFA) to produce the intermediate bilane. The acidolysis of dipyrromethanes and bilanes is avoided during a short period of time only if the dipyrromethane unit bears a sufficiently strong electron withdrawing group.

Using these experimental conditions and starting from EDPM, we were able to prepare up to 15 new corrole free bases bearing two ester groups on the 5 and 15 *meso* positions with yields ranging from 2 to 8% (Scheme 1). The use of such compounds in applied research area would require improved synthetic yields but their moderate values are still promising and comparable to the ones of the rare examples of corroles bearing one or multiple *meso* alkyl chains (0.6-5%) or a single *meso* ester group (6-20%).^[6g,25] The absence of detectable scrambling was the first piece of evidence of the strong electron withdrawing character of the 5,15-*meso* ester groups which is outlined by the stability of all compounds in solution even when a strong electron donating aryl group or a long alkyl chain occupies the remaining *meso* position. The high stability towards oxidation of the diester corrole derivatives was also illustrated when paraformaldehyde was used to prepare the disubstituted corrole **10** since no *meso-meso* linked corrole dimer was formed.^[26]

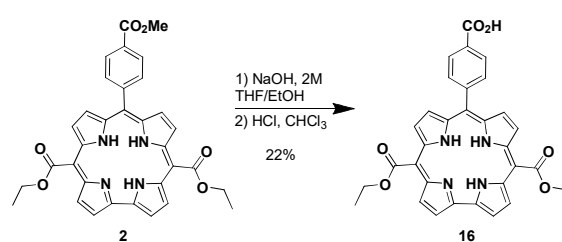
All the compounds were characterized by mass spectrometry, UV-Visible and ¹H NMR spectroscopy analyses. In the latter case, some interesting features have to be mentioned. For example, the aromatic induced magnetic field has an effect on the *meso* alkyl chains of compounds **11-15** where the signals of the four methylene (CH₂) fragments close to the macrocycle are well separated and shielded from those of the rest of the chain (See the Supporting Information). The ¹H NMR spectrum of the *meso*-triestercorrole **9** features two distinct quadruplets located at 4.84 and 4.93 ppm in a 2:1 ratio corresponding to the three methylene CH₂ groups of the ester substituents. This resonance split reflects the symmetry of the corrole which renders the central *meso* 10 position and the symmetrical 5,15 positions chemically non-equivalent. This differentiation was recently illustrated by the electrochemical study of the copper *meso*-triferrocenylcorrole where the middle ferrocenyl (Fc) group is oxidized at a higher potential compared to the oxidation of the symmetrical Fc groups.^[27] No supplementary corrole tautomerism involving the acidic phenolic hydrogen atom and producing an oxocorrogen derivative substituted by an semiquinone group was detected in the ¹H NMR and the UV-

Visible spectra of corrole **8** bearing a single (4-hydroxy-3,5-*tert*-butylphenyl) group (see the Supporting Information).^[28]



R	Corrole	Yield
C ₆ F ₅	1	5%
4-(CO ₂ Me)-C ₆ H ₄	2	8%
4-NO ₂ -C ₆ H ₄	3	4%
4-Me-C ₆ H ₄	4	8%
3,5-fBu ₂ -C ₆ H ₃	5	6%
4-MeO-C ₆ H ₄	6	7%
4-OH-C ₆ H ₄	7	3%
4-OH-3,5-fBu ₂ -C ₆ H ₃	8	6%
CO ₂ Et	9	2%
H	10	2%
C ₁₂ H ₂₅	11	3%
C ₁₃ H ₂₇	12	7%
C ₁₄ H ₂₉	13	7%
C ₁₅ H ₃₁	14	6%
C ₁₆ H ₃₃	15	6%

Scheme 1. Synthesis of 5,15-diester corroles 1-15.



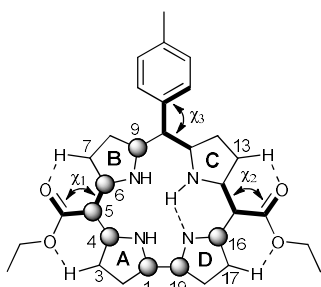
Scheme 2. Partial saponification of corrole **2**.

Despite the numerous different experimental conditions that were inspected, the saponification of corroles **1**, **4**, **9** and **10** did not give the expected corresponding 5,5-dicarboxycorrole derivatives but only caused the complete conversion of the starting material into compounds, although being of intense colors, that could not be isolated in pure form and identified. When basic conditions were applied to a solution of corrole **2**, we could isolate the compound **16** where the saponification only

occurred at the ester group born by the *meso* aryl substituent (Scheme 2). It was shown previously that the unsubstituted porphine can be obtained when a *meso* tetraesterporphyrin is submitted to strong acidic conditions.^[29] In our hands, such experimental conditions produced only the partial or complete disappearance of the starting *meso* ester corroles.

Crystal structure of corroles **2**, **4**, **6**, **9** and **15**

The slow diffusion of *n*-heptane into concentrated dichloromethane solutions of **2**, **4**, **6**, **9** and **15** yielded well diffracting single crystals suitable for an X-ray structure analysis (Figure 1 and Figure S1 in the Supporting Information). Details of the experimental structure determinations are given in the Supporting Information with the structural data (Table S1 and S2). Two structurally similar but crystallographically independent molecules of **4** are found in the corresponding asymmetric unit while those of **2**, **6**, **9** and **15** consist of a single corrole molecule. The five different structures show the presence of a unique and identical tautomeric form of the corrole free bases where the imino nitrogen is born by one of the two directly connected pyrrole units. A meticulous analysis of the corroles packing modes shows that the three inner hydrogen atoms are involved in intra- or intermolecular interactions. These structural properties will be here described using a numbering scheme of Maes *et al.* who published recently a detailed investigation on the fast NH tautomerization occurring in *meso*-pyrimidylcorrole derivatives (Scheme 3).^[30]



Scheme 3. Schematic drawing of **2** representing the numbering scheme of corroles used during the structural analyses and the intramolecular hydrogen bonds (Grey balls are placed on the carbon atoms C1, C4, C5, C6, C9, C16 and C19 used to define the mean plane of the macrocycles).

The imino nitrogen, located at position 24 and born by the pyrrole ring D will be named N_D. The notations N_A, H_A, N_B, H_B, N_C and H_C will correspond to the inner nitrogen and hydrogen atoms of the rings A, B and C. The seven carbon atoms C1, C4, C5, C6, C9, C16 and C19 will be used to define the macrocycle mean planes because it was shown that they are practically in the same plane for both NH interconverting tautomers of corrole derivatives.^[30d]

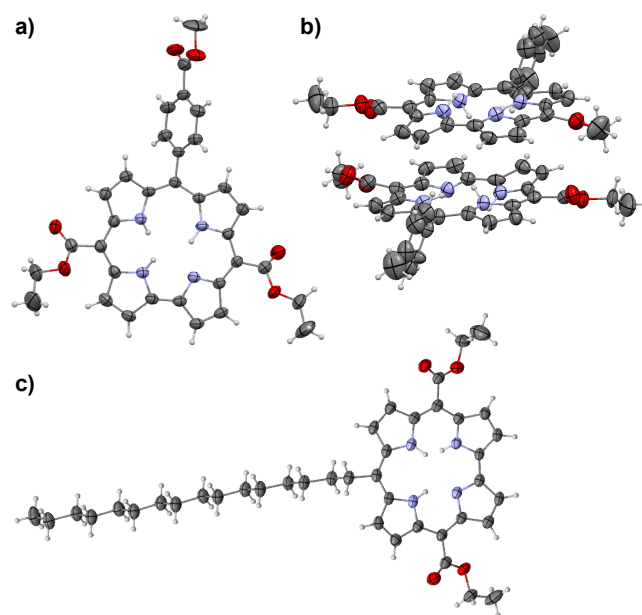


Figure 1. Ortep views of the asymmetric units of corroles a) **2**, b) **4** and c) **15**. The corresponding views of corroles **6** and **9** are reported in the SI.

As reported earlier in the few corrole free bases structures,^[4c,14b,25a,31] the aromatic macrocycles of the five compounds **2**, **4**, **6**, **9** and **15** are deformed from planarity due to the steric hindrance of the three internal protons. This steric repulsion is particularly effective between the pyrrole units A and B which are tipped alternatively above and below the macrocycle mean planes by angles ranging from 8 to 18°. The average value of the dihedral angles θ_1 between the rings A and B reaching 17° illustrates the H_A⋯H_B repulsions which produce in addition an out of plane deviation of H_A and H_B from their respective pyrrole units A and B (Average dihedral C5-C4-N_A-H_A angle of 28° and average dihedral angle C5-C6-N_B-H_B of 29°). The highest out of plane deviations of H_B result from the additional steric repulsion between H_B and H_C born by the rings B and C which are, in four structures, the most coplanar pyrrole units with a dihedral angle θ_2 ranging from 7 to 15°. The third kind of inner hydrogen atoms H_C are less deviated and are located close to the mean plane defined by the rings C and D which form a dihedral angle averaging 11°. These two rings are usually presented as the most coplanar pyrrole units due to their participation in intramolecular hydrogen bonds occurring between the hydrogen atoms H_C and the imino nitrogen atoms N_D. These moderate strength hydrogen bonds^[32] have mainly an electrostatic character and are responsible of the larger N_C-H_C distances averaging 1.14 Å while the shorter N_A-H_A and N_B-H_B average distances are 1.01 Å and 1.05 Å respectively (Table 1). It was shown recently that the N_C-H_C⋯N_D system forms an unsymmetrical proton sponge resulting in the faster existing corrole NH tautomerization process.^[33]

The low steric hindrance of the 5,15 *meso* ester groups is put into evidence by the low values of the torsion angles χ_1 and χ_2 which range from 10 to 24° (Table 1) while values higher that

36° were observed if the 5,15 ester groups are replaced by aryl substituents in *meso* triarylcorrole free bases.^[4c,14b,25a,31b-c] In *meso* triarylcorrole derivatives, the steric repulsion between the ortho substituents of the *meso* aryl group and the neighboring β -hydrogen atoms is always higher for the group placed at the central 10 *meso* position and results in higher χ_3 values. The same trend is observed in the five molecular structures of **2**, **4**, **6**, **9** and **15** where the central *meso* position is occupied either by an aryl group, an alkyl chain or a third ester group featuring χ_3 values higher than 60°. This value reaches 79° in **9** and is more than three times higher than the ones of the corresponding χ_1 and χ_2 . This feature is due to the lack of π -conjugation between the *meso* 10 substituent and the aromatic corrole ring while the orientation of the two other *meso* ester groups should facilitate such π -overlapping.

The low values of the dihedral angles χ_1 and χ_2 between the ester groups and the corrole moieties allow their participation in weak intramolecular hydrogen bonds of type C-H \cdots O with the neighboring β -hydrogen atoms (Scheme 3). The five structures of corroles **2**, **4**, **6**, **9** and **15** show an almost identical orientation of the 5,15 *meso* ester groups respective to the macrocycle. In each compound, the two carbonyl groups are placed on one side of the corrole ring and are both tilting towards the northern part (A,B) of the macrocycle since they interact with the β -hydrogen atoms born by C7 and C13 (Scheme 3). These weak interactions are accompanied on the other side of the corrole ring by the resulting weak hydrogen bonds occurring between the sp^2 ester oxygen atoms and β -hydrogen atoms born by C3 and C17 (Scheme 3).

An examination of the five crystals packings reveals that the corrole molecules are stacked into columns along the *a* axes. These columns can be described as assemblies of corrole dimers where two macrocycles are stacked head-to-tail in an anti-parallel fashion such that the pyrrole rings A and B of one molecule fall on the ring C and D of the other and vice versa (Figure 2). Consequently, the imino nitrogen atom N_D of one

macrocycle and the hydrogen atom H_{A'} of the other dimer half are forming two identical intermolecular hydrogen bonds characterized by N_A \cdots N_{D'} distances ranging from 3.131(3) to 3.241(4) Å and N_A-H_{A'} \cdots N_{D'} angles varying between 135 and 142° (Table 2). These two moderately long and symmetrical hydrogen bonds within a N_AH_{A'} \cdots N_{D'} dimer result in short intermacrocycle distances close to 3.25 Å (Table 2). A similar intermolecular hydrogen bond of type N_BH_{B'} \cdots N_{D'} occurs within the crystal packing of 5,10,15-tris(heptafluoropropyl)corrole where the low steric hindrance of the substituents allow a short intermacrocycle distance.^[25a] Moreover, it has to be noted that the formation of such N_AH_{A'} \cdots N_{D'} corrole dimers was considered as the possible source of an intermolecular corrole NH tautomerization process based on two simultaneous proton transfers occurring between the nitrogen N_A of one macrocycle and the nitrogen N_{D'} of another one.^[33]

The short intermacrocycle distances are the consequences of two supplementary structural features. The first one is the distribution of the two *meso* 10 substituents at opposite sides of the dimer which prevents their sterical repulsion. The second one is the nearly coplanar orientation of the 5,15 *meso* ester groups towards the macrocycle which facilitates the intermolecular approach despite their spatial proximity. The sp^2 nitrogen atom N_{D'} of each corrole is interacting with two different hydrogen atoms H_{C'} and H_A. In the latter case, the hydrogen atom H_A has an intermediate location between the N_{D'} lone pair and the p_z atomic orbital of N_{D'}. Therefore, it is possible to assume that both the lone pair of N_{D'} and the ring D π -system (through a NH \cdots π interaction as indicated here after) are contributing to the N_AH_{A'} \cdots N_{D'} intermolecular interactions. These two concomitant contributions were used previously to describe the interaction between the sp^2 nitrogen atom of a guanine and two hydrogen atoms of water molecules.^[34]

Table 1. Intramolecular geometrical and structural parameters of corroles **2**, **4**, **6**, **9** and **15** (DFT computed values are italicized).

	χ_1	χ_2	χ_3	$\theta_1^{[a]}$	$\theta_2^{[a]}$	$\theta_3^{[a]}$	$\theta_4^{[a]}$	N _A -H _A	N _B -H _B	N _C -H _C	N _D \cdots N _C (Å)	N _C -H _C \cdots N _D (°)
2	20	20	67	16	9	11	14	1.054	1.045	1.071	2.571(4)	138
	<i>18</i>	<i>32</i>	<i>62</i>	<i>24</i>	<i>17</i>	<i>14</i>	<i>19</i>	<i>1.003</i>	<i>1.007</i>	<i>1.020</i>	<i>2.614</i>	<i>132</i>
4 ^[b]	24	24	71	17	7	12	16	1.005	1.043	1.192	2.579(9)	143
	24	22	74	17	7	12	15	1.005	1.042	1.173	2.575(8)	143
	<i>18</i>	<i>31</i>	<i>62</i>	<i>24</i>	<i>17</i>	<i>14</i>	<i>19</i>	<i>1.003</i>	<i>1.007</i>	<i>1.020</i>	<i>2.615</i>	<i>132</i>
6	10	24	61	19	15	12	17	1.044	1.108	1.166	2.577(4)	128
	<i>16</i>	<i>32</i>	<i>61</i>	<i>24</i>	<i>19</i>	<i>15</i>	<i>19</i>	<i>1.003</i>	<i>1.007</i>	<i>1.020</i>	<i>2.615</i>	<i>132</i>
9	21	22	79	16	7	9	15	0.986	1.016	1.108	2.574(6)	134
	<i>20</i>	<i>34</i>	<i>48</i>	<i>23</i>	<i>15</i>	<i>13</i>	<i>19</i>	<i>1.003</i>	<i>1.007</i>	<i>1.020</i>	<i>2.617</i>	<i>132</i>
15 ^[c]	21	21	83	19	10	12	17	0.975	1.032	1.115	2.577(3)	145
	<i>19</i>	<i>32</i>	<i>84</i>	<i>23</i>	<i>15</i>	<i>12</i>	<i>19</i>	<i>1.003</i>	<i>1.007</i>	<i>1.020</i>	<i>2.618</i>	<i>132</i>

[a] Dihedral angle between pyrrole mean planes A and B (θ_1), B and C (θ_2), C and D (θ_3), A and D (θ_4). [b] Two slightly different molecules of **4** are present in the asymmetric unit. [c] χ_3 is here measured using the first two carbon atoms of the alkyl chain.

The five crystal packings can be described as assemblies of $N_A H_A \cdots N_{D'}$ corrole dimers into columns thanks to multiple inter-dimer interactions. One of these interactions involves the hydrogen atoms H_B . In the crystal structures of **2**, **4**, **9** and **15**, the two N_B-H_B bonds of a corrole dimer are oriented towards the rings D' of the two neighboring dimers and vice et versa (Figure 2 and Figure S2 in the Supporting Information). The projection of H_B on the interacting ring D' shows that the N_B-H_B bond is interacting with the C18'-C19' bond. In 1997, a wide range of $N-H \cdots \pi$ interactions observed in the Cambridge Structural Database were classified by Malone *et al.* into six different geometric types according to the values of five geometric parameters $d_{\pi D H}$, θ , α and d (Scheme 4).^[35] The first one ($d_{\pi D H}$) is the distance between the hydrogen atom H and the centroid of the aromatic ring π_D . α is the angle formed by the N-H bond and the $(\pi_D H)$ line which forms the angle θ with the aromatic ring mean plane. d is the horizontal distance given by $d_{\pi D H} \cos \theta$. The d critical value of 1.4 Å was extracted from the radius of a benzene ring viewed as circular. Therefore it cannot be fully respected when a pyrrole unit is involved. With the exception of d , the values of the geometric parameters $d_{\pi D H}$, θ and α are in accordance with a geometrical orientation of the N_B-H_B towards the interacting pyrrole unit D' following the type V which is the most common geometry of $N-H \cdots \pi$ (phenyl) interactions (Scheme 4 and Table 2). This spatial arrangement describes hydrogen atoms interacting with carbon atoms at the edge of the ring and which point to the carbon atom or to the ring centre.

The weak $N_B-H_B \cdots \pi$ interactions between $N_A H_A \cdots N_{D'}$ corrole dimers in the structures of **2**, **4**, **9** and **15** are replaced in the crystal packing of **6** by moderate intermolecular hydrogen bonds (Figure 2). In this particular case, each H_B atoms of a $N_A H_A \cdots N_{D'}$ corrole dimers (Mean planes distance of 3.23 Å) is interacting with the *meso* ester carbonyl group of a neighboring one resulting in a glide plane between two dimers and an inter-dimer distance of 3.87 Å. A similar hydrogen bond occurring between an inner hydrogen atom and the carbonyl group of ethyl acetate was identified in one crystal structure of *meso*-triphenylcorrole and was presented as the most likely factor in the solvent-dependent photophysical behavior of this corrole.^[14c,31c] The crystal structures of **2**, **4**, **6**, **9** and **15** show that the peripheral substitution of corrole free bases by unencumbered groups facilitates their intermolecular approach and gives rise to a self-association through $N-H \cdots \pi$ interactions or hydrogen bonds which was proposed recently during the measurement of corroles solvation energies.^[36]

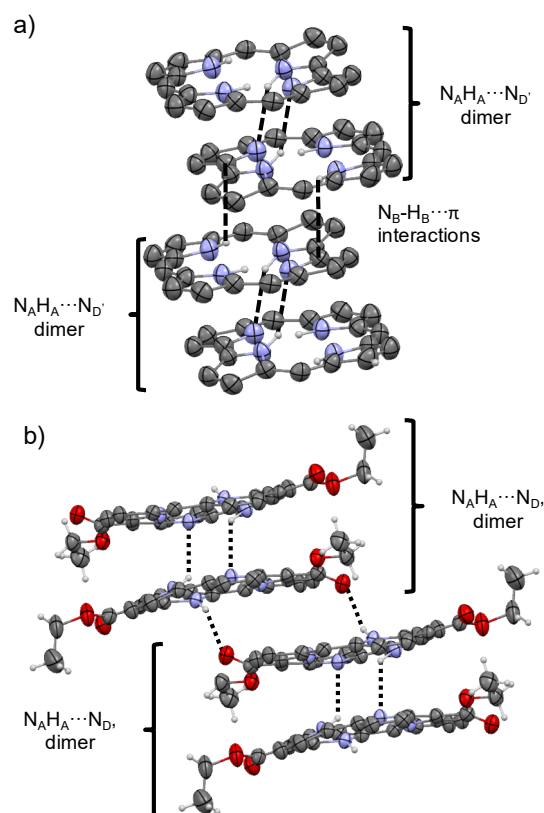
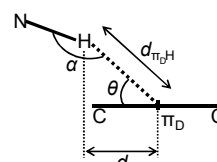


Figure 2. a) Intermolecular $N_A H_A \cdots N_{D'}$ hydrogen bonds and $N_B-H_B \cdots \pi$ interactions occurring within the crystal packing of corrole **9** (β -hydrogen atoms and *meso* ester groups are omitted for clarity); b) $N_A H_A \cdots N_{D'}$ and $N_B-H_B \cdots O=C$ intermolecular hydrogen bonds occurring within the crystal packing of corrole **6** (β -hydrogen atoms and *meso* aryl groups are omitted for clarity).



Scheme 4. Description parameters of $N-H \cdots \pi$ (phenyl) interaction.^[35] Type V: $d_{\pi D H} \leq 4.0 \text{ \AA}$, $\theta \leq 90^\circ$, $90^\circ \leq \alpha \leq 180^\circ$, $d > 1.4 \text{ \AA}$.

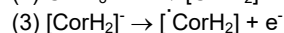
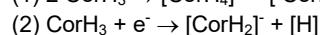
Table 2. Intermolecular geometrical and structural parameters of corroles **2**, **4**, **6**, **9** and **15**.

	N _A H _A ⋯N _D ' dimers parameters			Inter-dimers interactions						
	Mean planes distance (Å)	N _A ⋯N _D ' (Å)	N _A -H _A ⋯N _D ' (°)	Mean planes distance (Å)	d _{π_DH} (Å)	d (Å)	θ (°)	α (°)	N _B ⋯O=C (Å)	N _B -H _B ⋯O=C (°)
2	3.23	3.160(4)	142	3.57	3.29	1.12	70	98	-	-
4 ^[a]	3.25	3.152(9)	135	3.33 ^[b]	3.28	1.37	65	104	-	-
	3.26	3.148(9)	135		3.28	1.34	66	104	-	-
6	3.23	3.241(4)	141	3.87	-	-	-	-	2.919(4)	139
9	3.27	3.216(6)	136	3.72	3.26	0.88	74	112	-	-
15	3.25	3.131(3)	139	3.66	3.01	0.57	79	119	-	-

[a] Two slightly different molecules are present in the asymmetric unit. [b] Since the mean planes are not parallel but slightly tilted with 0.64°, this distance is measured between two centroids defined by C3, C6, C14, C17.

Electrochemical analyses of 5,15-diesteracorroles

The redox properties of 5,15-diesteracorroles were analyzed through the cyclic voltammograms (CV) of corroles **1-10**, **12** and **13** recorded in dichloromethane containing 0.1 M of [(ⁿBu₄N)PF₆]. The CVs recorded for corroles **4** and **9** are shown as typical examples in Figure 3. All the corresponding oxidation and reduction half-wave potential values ($E_{1/2}$) are listed in Table 3 together with those of 5,10,15-tris(pentafluorophenyl)corrole (**Tpfc**), 5,10,15-tris(4-methylphenyl)corrole (**TTc**)^[37] and 10-(4-methylphenyl)-5,15-(pentafluorophenyl)corrole (**C3**) measured within the same experimental conditions.^[38] Each CV features two irreversible reduction waves and up to three irreversible oxidation waves (Figure 3). Previous studies of the electrochemical properties of corrole free bases have shown that their redox behaviors are rather complicated since the starting compounds written as CorH₃ undergo a facile gain or loss of inner protons.^[37-39] Consequently, the effect of *meso*-ester substituents on the redox properties of corrole are here analyzed through the values of the half-wave potentials of the first oxidation and reduction processes which produce, according to equations 1 and 2, the corresponding radical [CorH₂], protonated [CorH₄]⁺ or deprotonated [CorH₂]⁻ forms which can be further oxidized or reduced.^[37-39] For each compound, we have also measured the half-wave potential value of the oxidation wave observed when reversing the scan in a positive direction just after the first reduction process producing the anion [CorH₂]⁻ (Figure 3). A new oxidation process corresponding to the redox couple [CorH₂]⁻/[CorH₂] (Equation (3)) is then detected at potentials ranging from -0.09 to 0.42 V/SCE (Table 3).^[37]



The replacement of the 5,15 pentafluorophenyl groups of **Tpfc** and **C3** into ester groups in **1** and **4**, leads to a positive shift of all the redox half-wave potentials (Table 3). This positive shifts ranging from 50 to 600 mV proves that the strong electron-withdrawing character of ester substituents is even higher than the one of pentafluorophenyl groups when they are born by the 5 and 15 *meso* positions. On the other hand, a little cathodic shift of the reduction potentials occurs when the *meso* 10 pentafluorophenyl group of **1** is replaced by a third ester group in **9**. The different impact of the *meso* 10 ester substituent can be explained by its nearly perpendicular orientation towards the macrocycle. Such orientation cannot allow the π-conjugation with the macrocycle which is probably effective for the two nearly co-planar 5 and 15 *meso* ester groups and explains their strong impact on the corrole electrochemical properties. An identical relationship between the π-conjugation and the anodic shift of redox potential values was described when one or two nitro groups were introduced at β positions of **TTc**.^[37]

If the corrole **1** is set apart, the nature of the *meso* 10 substituent has a low impact on the electrochemical properties of corroles. For example, the first oxidation process located at 0.78 V/SCE for the *meso* free derivative **10** is shifted by less than 50 mV along the **2-10** and **12-13** series. The same little variation is affecting the second oxidation process which has a potential value ranging from 1.03 to 1.31 V/SCE. Nevertheless, the $E_{1/2}$ oxidation values are still increasing with the electron-withdrawing character of the *meso* 10 substituent. This relationship is not fully respected by the $E_{1/2}$ value of the first reduction process. This contradiction arises from the uncertainties accompanying the complex determination of the $E_{1/2}$ values corresponding to very broad waves in the CV. However, when the anions produced by the first reduction are oxidized, the $E_{1/2}$ values are again increasing with the electron withdrawing properties of the central peripheral substituent. These results show that numerous substituents or functional groups can be introduced at the *meso* 10 position while preserving the stability against oxidation exerted by the 5,15 ester groups. Consequently, 5,15 ester corrole derivatives can

be used to prepare stable and sophisticated corrole based structures built through the derivatization of the *meso* 10 position.

Table 3. Half-wave potentials (V vs SCE) of corroles **1-10**, **12-13**, **C3**, **Ttc** and **Tpfc** measured in CH₂Cl₂ containing 0.1M of [(¹⁸Bu₄N)PF₆] (Scan rate of 100 mV/s).

	R10	R5,R15	Reduction		Oxidation			
			second	first	first	second	third	
Tpfc	C ₆ F ₅	C ₆ F ₅	-1.68	-0.81	0.35 ^[a]	0.88	1.25	1.78
Ttc ^[b]	4-CH ₃ -C ₆ H ₄	4-CH ₃ -C ₆ H ₄		-1.40	-0.09 ^[a]	0.33		
C3 ^[c]	4-CH ₃ -C ₆ H ₄	C ₆ F ₅			0.69			
1	C ₆ F ₅	CO ₂ Et	-1.44	-0.76	0.42 ^[a]	1.02	1.78	-
2	4-CO ₂ CH ₃ -C ₆ H ₄	CO ₂ Et	-1.49	-0.76	0.28 ^[a]	0.78	1.12	1.83
3	4-NO ₂ -C ₆ H ₄	CO ₂ Et	-1.59 ^[d]	-0.69 ^[d]	0.36 ^[a]	0.81	1.19	1.61
4	4-CH ₃ -C ₆ H ₄	CO ₂ Et	-1.51	-0.80	0.27 ^[a]	0.73	1.13	1.55
5	3,5- <i>t</i> Bu ₂ -C ₆ H ₃	CO ₂ Et	-1.51	-0.70	0.28 ^[a]	0.77	1.13	1.68
6	4-OCH ₃ -C ₆ H ₄	CO ₂ Et	-1.48	-0.60	0.27 ^[a]	0.74	1.06	1.47
7	4-OH-C ₆ H ₄	CO ₂ Et	-1.41	-0.46	0.27 ^[a]	0.77	1.08	-
8	4-OH-3,5- <i>t</i> Bu ₂ -C ₆ H ₃	CO ₂ Et	-1.53	-0.85	0.22 ^[a]	0.74	1.03	-
9	CO ₂ Et	CO ₂ Et	-1.46	-0.76	0.36 ^[a]	0.78	1.31	1.82
10	H	CO ₂ Et	-1.43	-0.49	0.38 ^[a]	0.78	1.09	-
12	C ₁₃ H ₂₇	CO ₂ Et	-1.55	-0.82	0.28 ^[a]	0.80	1.18	1.53
13	C ₁₄ H ₂₉	CO ₂ Et	-1.58	-0.75	0.22 ^[a]	0.76	1.16	1.83

[a] This redox couple can only be seen on the positive potential sweep after scanning through the first reduction. [b] From ref^[37]. [c] From ref^[38]. [d] Two reduction peaks of the nitro group are placed at -0.47 and -1.23 V vs SCE.

Photophysical properties of 5,15-diesteracorroles

The absorption and corrected emission spectra of corroles **Tpfc** and **1-16** recorded in dichloromethane are shown in Figures 4, S3, S4 and S5 (See the Supporting Information). The absorption maxima of all compounds and their molar absorption coefficients are collected in Table 4 together with the corresponding emission maxima (excitation at 570 nm), fluorescence quantum yields and lifetimes, radiative and nonradiative decay rates. All corroles exhibit a typical and intense Soret-type band located between 408 and 423 nm and three Q bands in the 500-650 nm domain. A fourth and very weak Q band was detected for the reference compound **Tpfc** for which our photophysical data are very similar to the ones measured by Ding *et al.* in the same experimental conditions.^[14c]

When the 5,15 pentafluorophenyl groups of **Tpfc** are changed into ester groups in **1**, the absorption bands are red

shifted by 1 to 18 nm. On the other hand, the absorption spectrum of **9** bearing a third and perpendicularly oriented *meso* ester ester group is almost identical to the UV-Visible spectrum of **1**. These results show again the higher impact of the 5,15 *meso* ester ester groups that are tightly coupling with the aromatic macrocycle and are responsible of these red-shifted absorption. A similar bathochromic shift was observed when the three *meso* phenyl groups of the 5,10,15-triphenylcorrole were replaced by thienyl moieties in *meso*-trithienylcorrole and was also attributed to their high degree of π -overlap with the corrole.^[40] When the *meso* free position of corrole **10** is substituted in compounds **1-9** and **11-16**, the shape of the UV-Visible spectrum is retained but a little supplementary red shift of all absorption bands is observed and is increasing with the electron donating properties of the third *meso* group (Figure 4 and Table 4). A similar effect of the electron donating and/or withdrawing properties of the *meso* substituents on the locations of the absorption bands was described in the *meso*-triarylcorrole series.^[14]

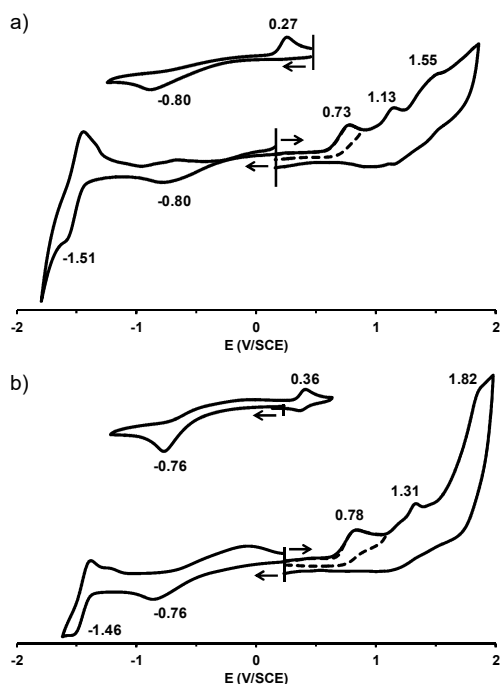


Figure 3. Cyclic voltammograms of corroles a) **4** and b) **9** in CH_2Cl_2 containing 0.1 M of $[\text{t}^{\text{Bu}}_4\text{N}]\text{PF}_6$ (Scan rate of 100 mV/s).

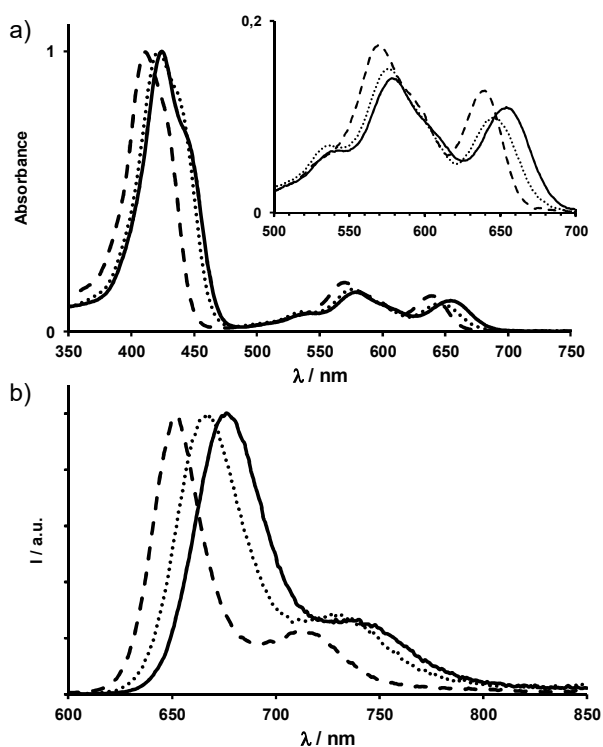


Figure 4. a) Normalized absorption spectra and b) Normalized corrected emission spectra (Excitation at 570 nm) of corroles **2** (dotted line), **8** (solid line) and **10** (dashed line) in aerated dichloromethane solutions at room temperature.

All corroles derivatives exhibit a relatively intense and structured emission, with fluorescence lifetimes in the nanosecond region (Table 4). Excitations in the Soret band domain (370-430 nm) or in the Q bands (550-700 nm) produced the same luminescence properties. The Stokes shifts ranging from 220 cm^{-1} for **Tpfc** to 543 cm^{-1} for **8** provide evidence that the electronic structures of the emitting states are quite different from the initially prepared Franck-Condon states. The introduction of 5,15 *meso* ester groups induces a red shift of the emission spectra which is enhanced by the electron-donating character of the group born by the third *meso* position. This bathochromic shift parallels the one observed in the absorption spectra (see above) and can be similarly explained. If corroles **3** and **9** are set apart, all corrole derivatives have a similar quantum yield close to 0.16 and a fluorescence lifetime in the range of 3-4 ns yielding a fluorescence rate in the range of $3\text{-}6 \times 10^7\text{ s}^{-1}$ and a rate constant for radiationless decay, k_{nr} , lower than $3 \times 10^8\text{ s}^{-1}$. Higher k_{nr} values were calculated for **3** and **9** which have also the lowest quantum yields and fluorescence lifetimes. The presence of intramolecular and non-fluorescent charge transfer (CT) states could enhance the radiationless decay. For example, a low-lying CT state involving a nitrophenyl group and stabilized in polar media was proposed to be responsible of the fluorescence quenching in nitro substituted *meso*-triarylcorroles derivatives.^[14b,14f] The formation of such CT state is here also supported by the recovery of the fluorescence intensity and excited state lifetime of corrole **3** when the polarity of the solvent is decreased by recording the fluorescence spectrum in toluene (Table 4). On the other hand, a lower solvent polarity did not affect the luminescence properties of **9** bearing a third *meso* ester group which can still produce fluorescence quenching CT states such as in tryptophan derivatives.^[41]

The photophysical properties of corroles are known to be solvent dependent and change dramatically when dimethylacetamide (DMAc) is used since a partial and/or complete deprotonation of the corrole could occur in very dilute solutions.^[14c] For example, the addition of triethylamine to a dichloromethane solution of corrole **6** increases the intensity of the Q band localized at 650 nm in the absorption spectrum whose shape is close to the one recorded in DMAc (Figure S6 in the supporting information). On the other hand, when TFA is added to a dilute solution of **6** in DMAc, the shape of UV-Visible spectrum is close to the one recorded in dichloromethane (Figure S6 in the supporting information). A detailed analysis of these intriguing solvent effects, which would require further investigations, is beyond the aim of the present study which focuses on the effects of the replacement of *meso* aryl substituents by *meso* ester groups.

Theoretical studies of 5,15-diester-corroles

The effects of the 5,15 *meso* ester groups on the structural, electronic and optical properties of corroles were theoretically investigated using DFT and TD-DFT methods. The geometry optimizations were performed without symmetry constrains in

the gas-phase and in dichloromethane and using the single crystal X-ray structures of corroles **2**, **4**, **6**, **9** and **15** as starting geometries. The optimized structures and calculated optical properties showed very little sensitivity to the used functional and solvation effects. We disclose here the results from the calculations performed in dichloromethane with the Gaussian 09 package,^[42] using hybrid B3LYP functionals in combination with triple- ζ def2-TZVPP basis set^[43] as reported earlier.^[37] Solvation effects were modeled during geometry optimizations and TD-DFT calculations using PCM (Polarizable Continuum Model) with the default IEFPCM (Integral Equation Formalism) variant as implanted in Gaussian 09.^[44]

The optimized structures of corroles **2**, **4**, **6**, **9** and **15** were calculated starting from their single crystal X-ray structures. Consequently, these calculated structures feature a single and identical corrole tautomeric form where the inner hydrogen atoms are located on the A, B and C pyrrole units. Several intramolecular geometrical parameters are listed in Table 1 and Table S3 together with the experimental values. The nature of the 10 *meso* substituent has a very little effect on the optimized geometry. For example, the dihedral angle θ_1 formed by the rings A and B is averaging 24°, while the corresponding angle θ_4 formed by the rings A and D is close to 19° for the five compounds (Table 1). These angles illustrate the steric repulsion between the inner hydrogen atoms that induces a significant macrocycle distortion from planarity which is higher than the one observed experimentally in the crystal structures where the crystal packings probably limit the amplitude of these out of plane deformations. The carbonyl groups of the 5 and 15 *meso* ester substituents are still placed on the same side of the corrole mean planes. The torsion angles χ_2 averaging 32° show that the *meso* 15 ester group has a less π -electronic communication with the corrole ring than the 5 ester moiety for which the torsion angles χ_1 averaging 18° are even lower than the experimental ones (Table 1). The torsion angle χ_3 of the third *meso* substituent are still higher than χ_1 and χ_2 , but decreases from 79 to 48° for the 10 *meso* ester group of **9** allowing a possible electronic communication with the aromatic macrocycle. The absence of any crystal packing and intermolecular interactions has consequences on the three inner N-H bonds which are now equal from one corrole to another. The intramolecular hydrogen bond between rings C and D is still effective since these two rings are the most coplanar and define a mean plane containing the hydrogen H_c.

The Kohn-Sham molecular orbital (MO) energies of the two highest occupied and the two lowest unoccupied molecular orbitals are listed in Table 5 and their plots are displayed in Figures 5 and S7 (See the Supporting Information). The HOMO energies of the five compounds are lower than -5.3 eV while the HOMO of **TTC**, calculated with the same functionals, was shown to be higher than -5.0 eV.^[37] Consequently, the replacement of the 5 and 15 *meso* p-methylphenyl groups of **TTC** by ester groups in **4** decreases the HOMO energy and illustrates the stabilizing effect of the *meso* ester groups towards oxidation. The impact of the third *meso* substituent on the MO energies is low with a HOMO-LUMO energy gap ranging from 2.45 eV in **2** to 2.59 eV in **9**.

The plots of the four MOs involved in the Gouterman 's model are shown in Figures 5 and S7. The HOMO of the five derivatives show a little contribution of the sp² carbon of the 5 *meso* ester group which is interacting with its parent *meso* carbon atom. Since the tautomerization process induces the equivalence of the two 5,15 *meso* ester groups, we can assume that the HOMO is delocalized slightly on both 5,15 *meso* ester groups as what is observed in the five LUMO which have large amplitudes on both groups. A similar delocalization with the 10 *meso* ester group of **9** is occurring in its LUMO+1 and could be the source of an intramolecular charge transfer responsible of the partial luminescence quenching.

Table 5. Calculated Kohn-Sham Orbital Energies of corroles **2**, **4**, **6**, **9** and **15** (eV).

MO	2	4	6	9	15
LUMO+1	-2.44	-2.45	-2.55	-2.64	-2.42
LUMO	-2.93	-2.93	-2.96	-3.00	-2.91
HOMO	-5.38	-5.41	-5.47	-5.59	-5.40
HOMO-1	-5.57	-5.57	-5.62	-5.67	-5.55

The ten lower electronic transitions of **2**, **4**, **6**, **9** and **15** were calculated by TD-DFT using the same functional/basis sets as used during optimization steps. The calculated excitation energies and oscillators strengths for the lowest excited states are reported in Tables 6 and S3 together with the major one-electron transitions contributing to the excited state solution vector (extracted using Gausssum 3.0 software^[46]). Each compound features two nearly degenerated and intense electronic transitions in the Soret Band domain and two weaker transitions in the Q bands region of the spectra. As observed experimentally, the electron donating properties of the 10 *meso* group induce a little red shift of the second Q band localized at 570 nm in the calculated spectrum of **9** and at 588 nm in the corresponding spectrum of **6** (Figure 6). According to the TD-DFT calculations, the third Q bands of corroles **1-16** localized around 640 nm are identified as vibrational in origin. The Gouterman 's model is still effective since the four corresponding MOs, HOMO-1, HOMO, LUMO and LUMO+1 are involved in the major contributions of the electronic transitions occurring in the visible domain (Table 6 and S3). For example, the LUMO+1 is involved in the four electronic transition of **9** occurring in the visible region and could be responsible of the quenching of its fluorescence (see above). A good correlation can be seen between the computed and experimental spectra of the five compounds even if only one tautomeric form of the corrole was taken into account during the TD-DFT calculations (Figures 6 and S8). It has to be noted, that a quite intense electronic transition around 380 nm was calculated for each derivative and was shown to involve mostly the HOMO-2 (**2**, **4**, **9** and **15**) and HOMO-3 (**6**) which are largely localized on the rings D or on the *meso* 10 aryl group. These transitions are probably the source of

the B bands enlargements towards the UV part of the light spectrum.

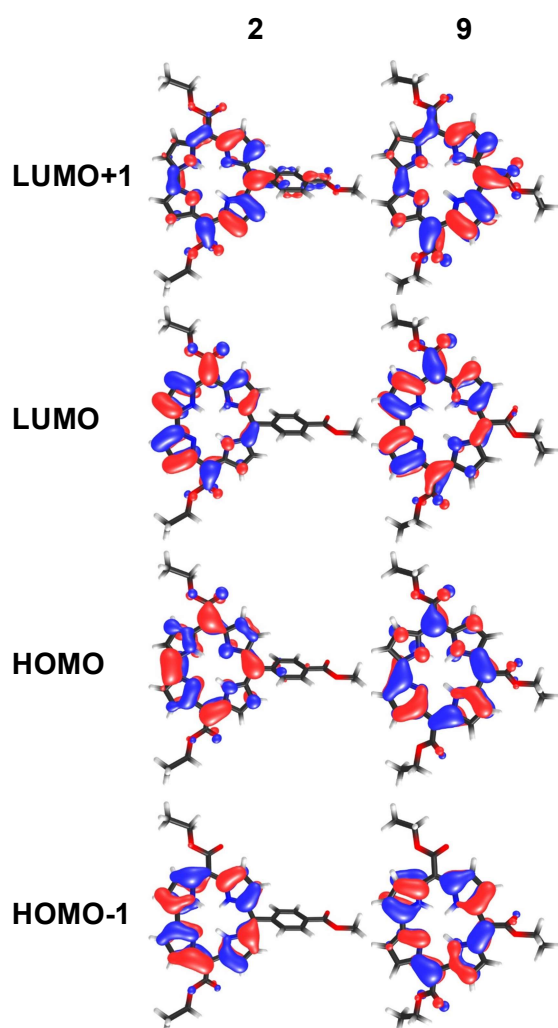


Figure 5. Plots of the frontier orbitals of corroles 2 and 9.

Conclusions

One strong limitation of the use of corrole free base derivatives in applied area of research is their sensitivity toward oxidative reagents or media. A common way to prevent corroles from oxidation is to introduce bulky electron withdrawing aryl groups on the peripheral *meso* positions. We described here that *meso* ester groups are a good alternative to stabilize corroles against oxidation and are, in this regard, even more effective than pentafluorophenyl groups. The low steric hindrance of peripheral ester moieties is illustrated by crystal packings featuring short intermacrocycle distances between corroles that are stacked into columns. Such supramolecular organizations are of major interest in building charge transport devices which are currently investigated. We have studied the physico-chemical properties

of sixteen 5,15 diesteracorrole derivatives where the *meso* 10 position is either free or occupied by various substituents including electron rich aryl groups and long alkyl chains. We have noticed that the nature of this group has a weak influence on the corroles physico-chemical properties and can even be a strong electron donating group without destabilizing the macrocycle if two strong electron withdrawing groups such as esters are placed on the 5 and 15 *meso* positions. This result opens the way to construct stable corrole free base superstructures built on the derivatization of the *meso* 10 position. Importantly, the introduction on the corrole skeleton of *meso* ester groups induces a red shift of the absorption and emission spectra but retains the fluorescence properties of the parent aromatic macrocycle which have to be kept in various applications such as imaging or the development of fluorescence based sensors. The strong electron withdrawing character of the *meso* ester groups is a new entry to tune the properties and the reactivity of metallocorroles derivatives and can thereby, for example, enhance their catalytic efficiency or Lewis acidity. Their impact on the properties of fluorescent phosphorus complexes is currently under study in our laboratory.

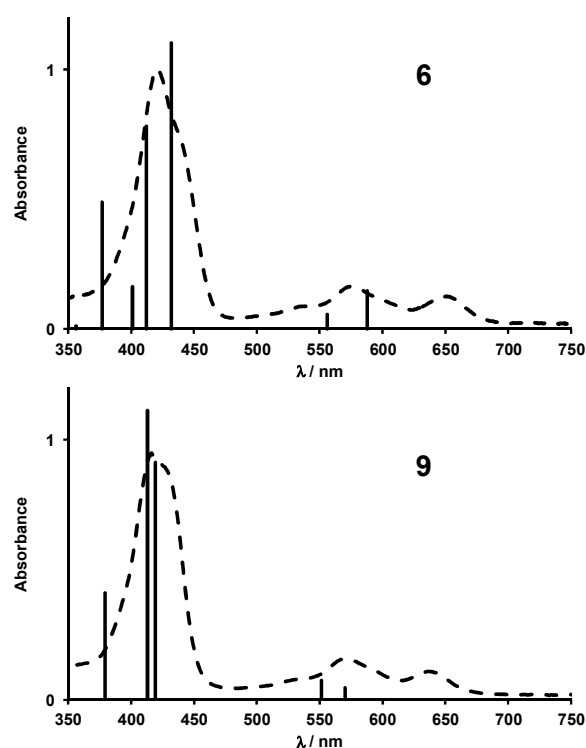


Figure 6. Comparison between computed and experimental absorption spectra of corroles 6 and 9 in dichloromethane.

Table 4. UV-Visible absorption and fluorescence data (of corroles **1-16** and **Tpfc** in aerated dichloromethane at 298 K.

	Absorption		Fluorescence					
	Soret band ^[a] λ_{\max}/nm ($\epsilon/10^4 \text{ M}^{-1} \text{ cm}^{-1}$)	Q bands λ_{\max}/nm ($\epsilon/10^4 \text{ M}^{-1} \text{ cm}^{-1}$)	$\lambda_{\max}^{[b]}/\text{nm}$	$\Phi_{\text{fl}}^{[c]}$	$\tau^{[d]}/\text{ns}$	$k_{\text{fl}}/10^7 \text{ s}^{-1}$	$k_{\text{nr}}/10^8 \text{ s}^{-1}$	
Tpfc	408 (11.40)	515 (0.59), 562 (1.81), 604 (0.95), 635 (0.18)	644, 702	0.16	4.61	3.5	1.8	
1	417 (11.28)	533 (0.65), 573 (1.69), 636 (1.04)	655, 717	0.165	4.13	4.0	2.0	
2	421 (11.79)	537 (0.82), 537 (1.74), 646 (1.16)	667, 729	0.15	3.20	4.7	2.7	
3	424 (7.45)	538 (0.72), 576 (1.48), 643 (0.90)	667, 730	0.11	2.44	4.5	3.6	
			668, 732 ^[e]	0.19 ^[e]	3.30 ^[e]	5.8 ^[e]	2.5 ^[e]	
4	421 (10.99)	534 (0.62), 576 (1.60), 648 (1.15)	669, 731	0.17	3.05	5.6	2.7	
5	421 (11.68)	536 (0.74), 577 (1.72), 651 (1.30)	668, 729	0.15	3.07 (3.15)	4.9	2.8	
6	421 (11.04)	537 (0.71), 577 (1.66), 651 (1.21)	674, 732	0.16	2.98	5.4	2.8	
7	421 (11.31)	536 (0.58), 578 (1.42), 650 (0.99)	673, 734	0.17	3.01	5.6	2.8	
8	423 (11.21)	538 (0.78), 578 (1.65), 653 (1.29)	677, 737	0.14	2.94	4.8	2.9	
9	418 (11.62)	534 (0.80), 571 (1.75), 638 (1.09)	655, 719	0.07	2.19 (2.56)	3.2	4.2	
			658, 722 ^[e]	0.075 ^[e]	2.24 ^[e]	3.3 ^[e]	4.1 ^[e]	
10	411 (11.01)	530 (0.60), 570 (1.92), 640 (1.39)	652, 713	0.16	3.92	4.1	2.1	
11	421 (11.56)	533 (0.52), 576 (1.65), 650 (1.25)	666, 730	0.175	3.02	5.8	2.7	
12	421 (11.21)	533 (0.59), 576 (1.69), 652 (1.28)	666, 730	0.165	3.02	5.5	2.8	
13	421 (11.31)	535 (0.62), 576 (1.69), 651 (1.30)	666, 730	0.17	3.03	5.6	2.7	
14	421 (10.99)	535 (0.62), 575 (1.65), 651 (1.25)	666, 730	0.165	3.04	5.4	2.7	
15	421 (11.17)	534 (0.63), 576 (1.66), 651 (1.25)	666, 730	0.16	3.02	5.3	2.8	
16	421 (10.80)	534 (0.65), 575 (1.61), 645 (1.10)	666, 728	0.15	3.22	4.7	2.6	

[a] The presence of a shoulder of the Soret band is detected for all compounds and is reported in the experimental part (SI). [b] λ_{\max} for the two bands derived from corrected emission spectra. [c] Luminescence quantum yields in air equilibrated dichloromethane, determined comparing corrected emission spectra and using TPP (tetraphenylporphyrin) in aerated toluene as a standard ($\Phi_{\text{fl}} = 0.11^{[45]}$). Excitation at 570 nm. [d] Fluorescence lifetimes in air equilibrated dichloromethane. Values obtained in air free dichloromethane are written between parentheses. [e] Corresponding values measured in aerated toluene.

Table 6. Composition, vertical excitation energies (nm) and oscillator strengths for the lowest optically allowed excited states of corroles **6** and **9**.

	States	E (nm)	<i>f</i>	Composition (%)
6	1 ¹ A	588	0.1468	HOMO→LUMO (66) HOMO-1→LUMO+1 (18) HOMO-1→LUMO (10)
	2 ¹ A	555	0.0554	HOMO-1→LUMO (56) HOMO→LUMO+1 (28) HOMO→LUMO (12)
	3 ¹ A	431	1.1029	HOMO→LUMO+1 (63) HOMO-1→LUMO (32)
	4 ¹ A	421	0.7818	HOMO-1→LUMO+1 (58) HOMO-2→LUMO (21) HOMO→LUMO (16)
	5 ¹ A	401	0.1643	HOMO-2→LUMO (63) HOMO-3→LUMO (26)
	6 ¹ A	376	0.4892	HOMO-3→LUMO (66) HOMO-2→LUMO (14) HOMO-1→LUMO+1 (11)
	7 ¹ A	356	0.0114	HOMO-2→LUMO+1 (96)
9	1 ¹ A	570	0.0448	HOMO-1→LUMO (51) HOMO→LUMO+1 (29) HOMO→LUMO (14)
	2 ¹ A	551	0.0741	HOMO→LUMO (57) HOMO-1→LUMO+1 (23) HOMO-1→LUMO (13)
	3 ¹ A	419	0.9123	HOMO→LUMO+1 (60) HOMO-1→LUMO (31)
	4 ¹ A	412	1.1125	HOMO-1→LUMO+1 (65) HOMO→LUMO (26)
	5 ¹ A	379	0.4103	HOMO-2→LUMO (82)

Acknowledgements

D. G. gratefully acknowledges the China Scholarship Council for financial support. F.-X.D. is supported by the FP7 Future and Emerging Technologies for Energy Programme through the project PEPDIODE.

Keywords: Corroles • Esters • Porphyrinoids • Electrochemistry • Luminescence

- [1] A. W. Johnson, I. T. Kay, *Proc. Chem. Soc.* **1964**, 89-90.
 [2] a) A. W. Johnson, I. T. Kay, *J. Chem. Soc.* **1965**, 1620-1629; b) R. L. N. Harris, A. W. Johnson, I. T. Kay, *Chem. Commun.* **1965**, 232-234; c) D. Dolphin, A. W. Johnson, J. Leng, P. Van den Broek, *J. Chem. Soc. (C)* **1966**, 880-884; d) J. Engel, A. Gossauer, *J. Chem. Soc., Chem.*

- Commun.* **1975**, 713-714; e) R. K. Pandey, H. Zhou, K. Gerzevske, K. M. Smith, *J. Chem. Soc., Chem. Commun.* **1992**, 183-185; f) R. K. Pandey, K. R. Gerzevske, H. Zhou, K. M. Smith, *J. Chem. Soc., Perkin Trans. 1* **1994**, 971-977; g) S. Neya, K. Ohyama, N. Funasaki, *Tetrahedron Lett.* **1997**, *38*, 4113-4116; h) S. Licocchia, M. L. Di Vona, R. Paolesse, *J. Org. Chem.* **1998**, *63*, 3190-3195; i) F. Jérôme, C. P. Gros, C. Tardieux, J.-M. Barbe, R. Guillard, *Chem. Commun.* **1998**, 2007-2008; j) R. Paolesse, in *The Porphyrin Handbook*, Vol. 2 (Eds.: K. M. Kadish, K. M. Smith, R. Guillard), Academic Press, New York, **2000**, pp. 201-232; k) R. Guillard, C. P. Gros, F. Bolze, F. Jérôme, Z. Ou, J. Shao, J. Fischer, R. Weiss, K. M. Kadish, *Inorg. Chem.* **2001**, *40*, 4845-4855; l) R. Guillard, F. Jérôme, J.-M. Barbe, C. P. Gros, Z. Ou, J. Shao, J. Fischer, R. Weiss, K. M. Kadish, *Inorg. Chem.* **2001**, *40*, 4856-4865; m) R. Guillard, J.-M. Barbe, C. Stern, K. M. Kadish, in *The Porphyrin Handbook*, Vol. 116 (Eds.: K. M. Kadish, K. M. Smith, R. Guillard), Elsevier New York, **2003**, pp. 201-232; n) J.-M. Barbe, C. Stern, E. Pacholska, E. Espinosa, R. Guillard, *J. Porphyrins Phthalocyanines* **2004**, *8*, 301-312.
 [3] a) N. M. Loim, E. V. Grishko, N. I. Pyshnograeva, E. V. Vorontsov, V. I. Sokolov, *Izv. Akad. Nauk. Ser. Khim.* **1994**, 925-927; b) E. Rose, A. Kossanyi, M. Quelquejeu, M. Soleilhavoup, F. Duwvran, N. Bernard, A. Lecas, *J. Am. Chem. Soc.* **1996**, *118*, 1567-1568.
 [4] a) R. Paolesse, L. Jaquinod, D. J. Nurco, S. Mini, F. Sagone, T. Boschi, K. M. Smith, *Chem. Commun.* **1999**, 1307-1308; b) Z. Gross, N. Galili, I. Saltsman, *Angew. Chem.* **1999**, *111*, 1530-1533; *Angew. Chem. Int. Ed.* **1999**, *38*, 1427-1429; c) Z. Gross, N. Galili, L. Simkhovich, I. Saltsman, M. Botoshansky, D. Bläser, R. Boese, I. Goldberg, *Org. Lett.* **1999**, *1*, 599-602.
 [5] J.-W. Ka, W.-S. Cho, C.-H. Lee, *Tetrahedron Lett.* **2000**, *41*, 8121-8125.
 [6] a) R. Paolesse, S. Nardis, F. Sagone, R. G. Khoury, *J. Org. Chem.* **2001**, *66*, 550-556; b) C. V. Asokan, S. Smeets, W. Dehaen, *Tetrahedron Lett.* **2001**, *42*, 4483-4485; c) D. T. Gryko, K. Jadach, *J. Org. Chem.* **2001**, *66*, 4267-4275; d) R. Guillard, D. T. Gryko, G. Canard, J.-M. Barbe, B. Koszarna, S. Brandès, M. Tasiar, *Org. Lett.* **2002**, *4*, 4491-4494; e) D. T. Gryko, K. E. Piechota, *J. Porphyrins Phthalocyanines* **2002**, *6*, 81-97; f) D. T. Gryko, B. Koszarna, *Org. Biomol. Chem.* **2003**, *1*, 350-357; g) D. T. Gryko, B. Koszarna, *Synthesis* **2004**, 2205-2209; h) G. R. Geier, III, J. F. B. Chick, J. B. Callinan, C. G. Reid, W. P. Auguscinski, *J. Org. Chem.* **2004**, *69*, 4159-4169; i) B. Koszarna, D. T. Gryko, *J. Org. Chem.* **2006**, *71*, 3707-3717; j) T. Rohand, E. Dolusic, T. H. Ngo, W. Maes, W. Dehaen, *ARKIVOC* **2007**, 307-324; W. Maes, T. H. Ngo, J. Vanderhaeghen, W. Dehaen, *Org. Lett.* **2007**, *9*, 3165-3168; k) R. P. Briñas, C. Brückner, *Synlett* **2001**, 442-444; l) A. Nowak-Król, R. Plamont, G. Canard, J. A. Edzang, D. T. Gryko, T. S. Balaban, *Chem. Eur. J.* **2015**, *21*, 1488-1498.
 [7] C. Erben, S. Will, K. M. Kadish, in *The Porphyrin Handbook*, Vol. 2 (Eds.: K. M. Kadish, K. M. Smith, R. Guillard), Academic Press, New York, **2000**, pp. 233-300.
 [8] a) E. Rabinovich, I. Goldberg, Z. Gross, *Chem. Eur. J.* **2011**, *17*, 12294-12301; b) A. B. Alemayehu, A. Ghosh, *J. Porphyrins Phthalocyanines* **2011**, *15*, 106-110.
 [9] A. L. Ward, H. L. Buckley, W. W. Lukens, J. Arnold, *J. Am. Chem. Soc.* **2013**, *135*, 13965-13971.
 [10] A. B. Alemayehu, H. Vazquez-Lima, C. M. Beavers, K. J. Gagnon, J. Bendix, A. Ghosh, *Chem. Commun.* **2014**, *50*, 11093-11096.
 [11] a) Z. Gross, H. B. Gray, *Adv. Synth. Catal.* **2004**, *346*, 165-170; b) K. M. Kadish, L. Frémond, Z. Ou, J. Shao, C. Shi, F. C. Anson, F. Burdet, C. P. Gros, J.-M. Barbe, R. Guillard, *J. Am. Chem. Soc.* **2005**, *127*, 5625-5631; c) I. Aviv, Z. Gross, *Chem. Commun.* **2007**, 1987-1999; d) I. Aviv-Harel, Z. Gross, *Chem. Eur. J.* **2009**, *15*, 8382-8394; e) A. N. Biswas, P. Das, A. Agarwala, D. Bandyopadhyay, P. Bandyopadhyay, *J. Mol. Catal. A: Chem.* **2010**, *326*, 94-98; f) D. K. Dogutan, S. A. Stoian, R. McGuire, M. Schwalbe, T. S. Teets, D. G. Nocera, *J. Am. Chem. Soc.* **2011**, *133*, 131-140; g) K. Nakano, K. Kobayashi, T. Ohkawara, H. Imoto, K. Nozaki, *J. Am. Chem. Soc.* **2013**, *135*, 8456-8459; h) H.-Y.

- Liu, M. H. R. Mahmood, S.-X. Qiu, C. K. Chang, *Coord. Chem. Rev.* **2013**, *257*, 1306-1333; i) M. Schmidlehner, F. Faschinger, L. M. Reith, M. Ertl, W. Schöfberger, *Appl. Organomet. Chem.* **2013**, *27*, 395-405; j) T. Kuwano, T. Kurahashi, S. Matsubara, *Chem. Lett.* **2013**, *42*, 1241-1243; k) C. Robert, T. Ohkawara, K. Nozaki, *Chem. Eur. J.* **2014**, *20*, 4789-4795.
- [12] a) R. Paolesse, C. Di Natale, A. Macagnano, F. Sagone, M. A. Scarselli, P. Chiaradia, V. I. Troitsky, T. S. Berzina, A. D'Amico, *Langmuir* **1999**, *15*, 1268-1274; b) C. Di Natale, R. Paolesse, A. Macagnano, V. I. Troitsky, T. S. Berzina, A. D'Amico, *Anal. Chim. Acta* **1999**, *384*, 249-259; c) J.-M. Barbe, G. Canard, S. Brandès, F. Jérôme, G. Dubois, R. Guillard, *Dalton Trans.* **2004**, 1208-1214; d) J.-M. Barbe, G. Canard, S. Brandès, R. Guillard, *Angew. Chem.* **2005**, *117*, 3163-3166; *Angew. Chem. Int. Ed.* **2005**, *44*, 3103-3106; e) J.-M. Barbe, G. Canard, S. Brandès, R. Guillard, *Chem. Eur. J.* **2007**, *13*, 2118-2129; f) L. Lvova, C. Di Natale, A. D'Amico, R. Paolesse, *J. Porphyrins Phthalocyanines* **2009**, *13*, 1168-1178; g) C. I. M. Santos, E. Oliveira, J. F. B. Barata, M. A. F. Faustino, J. A. S. Cavaleiro, M. G. P. M. S. Neves, C. Lodeiro, *Inorg. Chim. Acta* **2014**, *417*, 148-154; h) B. Basumatary, M. Ayoub Kaloo, V. Kumar Singh, R. Mishra, M. Murugavel, J. Sankar, *RSC Adv.* **2014**, *4*, 28417-28420.
- [13] a) H. Agadjanian, J. J. Weaver, A. Mohammed, A. Rentsendorj, S. Bass, J. Kim, I. J. Dmochowski, R. Margalit, H. B. Gray, Z. Gross, L. K. Medina-Kauwe, *Pharm. Res.* **2006**, *23*, 367-377; b) A. Haber, A. Mohammed, B. Fuhrman, N. Volkova, R. Coleman, T. Hayek, M. Aviram, Z. Gross, *Angew. Chem. Int. Ed.* **2008**, *47*, 7896-7900; c) L. Kupershmidt, Z. Okun, T. Amit, S. Mandel, I. Saltsman, A. Mohammed, O. Bar-Am, Z. Gross, M. B. H. Youdim, *J. Neurochem.* **2010**, *113*, 363-373; d) A. Haber, M. Aviram, Z. Gross, *Chem. Sci.* **2011**, *2*, 295-302; e) J.-T. Huang, X.-L. Wang, Y. Zhang, M. H. R. Mahmood, Y.-Y. Huang, X. Ying, L.-N. Ji, H.-Y. Liu, *Transition Metal Chem.* **2013**, *38*, 283-289; f) A. Haber, A. Abu-Younis Ali, M. Aviram, Z. Gross, *Chem. Commun.* **2013**, *49*, 10917-10919; g) X. Liang, J. Mack, L.-M. Zheng, Z. Shen, N. Kobayashi, *Inorg. Chem.* **2014**, *53*, 2797-2802.
- [14] a) R. Paolesse, F. Sagone, A. Macagnano, T. Boschi, L. Prodi, M. Montalti, N. Zaccheroni, F. Bolletta, K. M. Smith, *J. Porphyrins Phthalocyanines* **1999**, *3*, 364-370; b) R. Paolesse, A. Marini, S. Nardis, A. Froio, F. Mandoj, D. J. Nurco, L. Prodi, M. Montalti, K. M. Smith, *J. Porphyrins Phthalocyanines* **2003**, *7*, 25-36; c) T. Ding, E. A. Aleman, D. A. Modarelli, C. J. Ziegler, *J. Phys. Chem. A* **2005**, *109*, 7411-7417; d) B. Ventura, A. Degli Esposti, B. Koszarna, D. T. Gryko, L. Flamigni, *New J. Chem.* **2005**, *29*, 1559-1566; e) C. P. Gros, F. Brisach, A. Meristoudi, E. Espinosa, R. Guillard, P. D. Harvey, *Inorg. Chem.* **2007**, *46*, 125-135; f) F. Nastasi, S. Campagna, T. H. Ngo, W. Dehaen, W. Maes, M. Kruk, *Photochem. Photobiol. Sci.* **2011**, *10*, 143-150.
- [15] A. Haber, H. Agadjanian, L. K. Medina-Kauwe, Z. Gross, *J. Inorg. Biochem.* **2008**, *102*, 446-457.
- [16] a) L. Shi, H. Y. Liu, L. P. Si, K. M. Peng, L. L. You, H. Wang, L. Zhang, L. N. Ji, C. K. Chang, H. F. Jiang, *Chin. Chem. Lett.* **2010**, *21*, 373-375; b) L. Shi, H.-Y. Liu, K.-M. Peng, X.-L. Wang, L.-L. You, J. Lu, L. Zhang, H. Wang, L.-N. Ji, H.-F. Jiang, *Tetrahedron Lett.* **2010**, *51*, 3439-3442; c) W. Shao, H. Wang, S. He, L. Shi, K. Peng, Y. Lin, L. Zhang, L. Ji, H. Liu, *J. Phys. Chem. B* **2012**, *116*, 14228-14234.
- [17] a) C.-Y. Li, X.-B. Zhang, Z.-X. Han, B. Aakermark, L. Sun, G.-L. Shen, R.-Q. Yu, *Analyst* **2006**, *131*, 388-393; b) C.-L. He, F.-L. Ren, X.-B. Zhang, Z.-X. Han, *Talanta* **2006**, *70*, 364-369; c) A. Pariyar, S. Bose, S. S. Chhetri, A. N. Biswas, P. Bandyopadhyay, *Dalton Trans.* **2012**, *41*, 3826-3831; d) C. I. M. Santos, E. Oliveira, J. F. B. Barata, M. A. F. Faustino, J. A. S. Cavaleiro, M. G. P. M. S. Neves, C. Lodeiro, *J. Mater. Chem.* **2012**, *22*, 13811-13819.
- [18] a) L. Flamigni, D. T. Gryko, *Chem. Soc. Rev.* **2009**, *38*, 1635-1646; b) B. Bursa, D. Wróbel, K. Lewandowska, A. Graja, M. Grzybowski, D. T. Gryko, *Synth. Met.* **2013**, *176*, 18-25; c) Y. Wang, Z. Wang, X. Guo, R. Cui, X. Gao, S. Yang, F. Chang, J. Dong, B. Sun, *J. Nanosci. Nanotechnol.* **2014**, *14*, 5370-5374; d) C. Li, J. Zhang, X. Liu, Y. Zhou, D. Sun, P. Cheng, B. Zhang, Y. Feng, *RSC Adv.* **2014**, *4*, 40758-40762.
- [19] C. Tardieux, C. P. Gros, R. Guillard, *J. Heterocycl. Chem.* **1998**, *35*, 965-970.
- [20] C. P. Gros, J.-M. Barbe, E. Espinosa, R. Guillard, *Angew. Chem.* **2006**, *118*, 5770-5773; *Angew. Chem. Int. Ed.* **2006**, *45*, 5642-5645.
- [21] a) J. F. B. Barata, A. M. G. Silva, M. G. P. M. S. Neves, A. C. Tomé, A. M. S. Silva, J. A. S. Cavaleiro, *Tetrahedron Lett.* **2006**, *47*, 8171-8174; b) J. F. B. Barata, M. G. P. M. S. Neves, A. C. Tomé, M. A. F. Faustino, A. M. S. Silva, J. A. S. Cavaleiro, *Tetrahedron Lett.* **2010**, *51*, 1537-1540; c) S. Hirabayashi, M. Omote, N. Aratani, A. Osuka, *Bull. Chem. Soc. Jpn.* **2012**, *85*, 558-562.
- [22] S. Nardis, G. Pomarico, F. R. Fronczek, M. G. H. Vicente, R. Paolesse, *Tetrahedron Lett.* **2007**, *48*, 8643-8646.
- [23] a) R. Paolesse, S. Nardis, M. Stefanelli, F. R. Fronczek, M. G. H. Vicente, *Angew. Chem.* **2005**, *117*, 3107-3110; *Angew. Chem. Int. Ed.* **2005**, *44*, 3047-3050; b) F. Mandoj, M. Stefanelli, S. Nardis, M. Mastroianni, F. R. Fronczek, K. M. Smith, R. Paolesse, *Chem. Commun.* **2009**, 1580-1582; c) F. Mandoj, S. Nardis, G. Pomarico, M. Stefanelli, L. Schiaffino, G. Ercolani, L. Prodi, D. Genovese, N. Zaccheroni, F. R. Fronczek, K. M. Smith, X. Xiao, J. Shen, K. M. Kadish, R. Paolesse, *Inorg. Chem.* **2009**, *48*, 10346-10357; d) Y. Fang, F. Mandoj, S. Nardis, G. Pomarico, M. Stefanelli, D. O. Cicero, S. Lentini, A. Vecchi, Y. Cui, L. Zeng, K. M. Kadish, R. Paolesse, *Inorg. Chem.* **2014**, *53*, 7404-7415.
- [24] Y. Terazono, E. J. North, A. L. Moore, T. A. Moore, D. Gust, *Org. Lett.* **2012**, *14*, 1776-1779.
- [25] a) L. Simkhovich, I. Goldberg, Z. Gross, *J. Inorg. Biochem.* **2000**, *80*, 235-238; b) R. Goldschmidt, I. Goldberg, Y. Balazs, Z. Gross, *J. Porphyrins Phthalocyanines* **2006**, *10*, 76-86; c) B. Koszarna, R. Voloshchuk, D. T. Gryko, *Synthesis* **2007**, 1339-1342; d) K. E. Thomas, J. Conradie, L. K. Hansen, A. Ghosh, *Inorg. Chem.* **2011**, *50*, 3247-3251.
- [26] B. Koszarna, D. T. Gryko, *Chem. Commun.* **2007**, 2994-2996.
- [27] G. Pomarico, A. Vecchi, F. Mandoj, O. Bortolini, D. O. Cicero, P. Galloni, R. Paolesse, *Chem. Commun.* **2014**, *50*, 4076-4078.
- [28] Y. Xie, J. P. Hill, A. L. Schumacher, P. A. Karr, F. D'Souza, C. E. Anson, A. K. Powell, K. Ariga, *Chem. Eur. J.* **2007**, *13*, 9824-9833.
- [29] S. Neya, J. Quan, M. Hata, T. Hoshino, N. Funasaki, *Tetrahedron Lett.* **2006**, *47*, 8731-8732.
- [30] a) Y. B. Ivanova, V. A. Savva, N. Z. Mamardashvili, A. S. Starukhin, T. H. Ngo, W. Dehaen, W. Maes, M. M. Kruk, *J. Phys. Chem. A* **2012**, *116*, 10683-10694; b) M. Kruk, T. H. Ngo, P. Verstappen, A. Starukhin, J. Hofkens, W. Dehaen, W. Maes, *J. Phys. Chem. A* **2012**, *116*, 10695-10703; c) M. Kruk, T. H. Ngo, V. Savva, A. Starukhin, W. Dehaen, W. Maes, *J. Phys. Chem. A* **2012**, *116*, 10704-10711; d) W. Beenken, M. Presselt, T. H. Ngo, W. Dehaen, W. Maes, M. Kruk, *J. Phys. Chem. A* **2014**, *118*, 862-871.
- [31] a) H. R. Harrison, O. J. R. Hodder, D. C. Hodgkin, *J. Chem. Soc. (B)* **1971**, 640-645; b) R. Paolesse, S. Nardis, M. Venanzi, M. Mastroianni, M. Russo, F. R. Fronczek, M. G. H. Vicente, *Chem. Eur. J.* **2003**, *9*, 1192-1197; c) T. Ding, J. D. Harvey, C. J. Ziegler, *J. Porphyrins Phthalocyanines* **2005**, *9*, 22-27.
- [32] a) G. A. Jeffrey, *An Introduction to Hydrogen Bonding*, Oxford University Press, Oxford, **1997**; b) J. W. Steed, J. L. Atwood, *Supramolecular Chemistry*, Second ed., John Wiley & Sons, Ltd., Chichester, **2009**.
- [33] S. Szymański, P. Paluch, D. T. Gryko, A. Nowak-Król, W. Bocian, J. Sitkowski, B. Koszarna, J. Śniechowska, M. J. Potrzebowski, L. Kozerski, *Chem. Eur. J.* **2014**, *20*, 1720-1730.
- [34] O. S. Sukhanov, O. V. Shishkin, L. Gorb, J. Leszczynski, *Struct. Chem.* **2008**, *19*, 171-180.
- [35] J. F. Malone, C. M. Murray, M. H. Charlton, R. Docherty, A. J. Lavery, *J. Chem. Soc., Faraday Trans.* **1997**, *93*, 3429-3436.

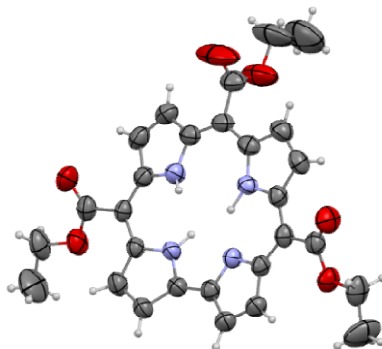
-
- [36] D. B. Berezin, D. R. Karimov, M. B. Berezin, *Russ. J. Phys. Chem. A* **2013**, *87*, 593-597.
- [37] M. Stefanelli, G. Pomarico, L. Tortora, S. Nardis, F. R. Fronczek, G. T. McCandless, K. M. Smith, M. Manowong, P. Chen, K. M. Kadish, A. Rosa, G. Ricciardi, R. Paolesse, *Inorg. Chem.* **2012**, *51*, 6928-6942.
- [38] R. Voloshchuk, D. T. Gryko, M. Chotkowski, A. I. Ciuciu, L. Flamigni, *Chem. Eur. J.* **2012**, *18*, 14845-14859.
- [39] a) J.-P. Gisselbrecht, M. Gross, E. Vogel, S. Will, *J. Electroanal. Chem.* **2001**, *505*, 170-172; b) J. Shen, J. Shao, Z. Ou, W. E. B. Koszarna, D. T. Gryko, K. M. Kadish, *Inorg. Chem.* **2006**, *45*, 2251-2265; c) Z. Ou, J. Shen, J. Shao, W. E. M. Galezowski, D. T. Gryko, K. M. Kadish, *Inorg. Chem.* **2007**, *46*, 2775-2786.
- [40] J. A. Greco, A. Rossi, R. R. Birge, C. Brückner, *Photochem. Photobiol.* **2014**, *90*, 402-414.
- [41] P. L. Muiño, P. R. Callis, *J. Phys. Chem. B* **2009**, *113*, 2572-2577.
- [42] Gaussian 09, Revision D.01, M. J. Frisch, G. W. Trucks, H. B. Schlegel, G. E. Scuseria, M. A. Robb, J. R. Cheeseman, G. Scalmani, V. Barone, B. Mennucci, G. A. Petersson, H. Nakatsuji, M. Caricato, X. Li, H. P. Hratchian, A. F. Izmaylov, J. Bloino, G. Zheng, J. L. Sonnenberg, M. Hada, M. Ehara, K. Toyota, R. Fukuda, J. Hasegawa, M. Ishida, T. Nakajima, Y. Honda, O. Kitao, H. Nakai, T. Vreven, J. A. Montgomery, Jr., J. E. Peralta, F. Ogliaro, M. Bearpark, J. J. Heyd, E. Brothers, K. N. Kudin, V. N. Staroverov, T. Keith, R. Kobayashi, J. Normand, K. Raghavachari, A. Rendell, J. C. Burant, S. S. Iyengar, J. Tomasi, M. Cossi, N. Rega, J. M. Millam, M. Klene, J. E. Knox, J. B. Cross, V. Bakken, C. Adamo, J. Jaramillo, R. Gomperts, R. E. Stratmann, O. Yazyev, A. J. Austin, R. Cammi, C. Pomelli, J. W. Ochterski, R. L. Martin, K. Morokuma, V. G. Zakrzewski, G. A. Voth, P. Salvador, J. J. Dannenberg, S. Dapprich, A. D. Daniels, O. Farkas, J. B. Foresman, J. V. Ortiz, J. Cioslowski, and D. J. Fox, Gaussian, Inc., Wallingford CT, 2013.
- [43] F. Weigend, R. Ahlrichs, *Phys. Chem. Chem. Phys.* **2005**, *7*, 3297-3305.
- [44] S. Miertuš, E. Scrocco, J. Tomasi, *Chem. Phys.* **1981**, *55*, 117-129.
- [45] P. G. Seybold, M. Gouterman, *J. Mol. Spectrosc.* **1969**, *31*, 1-13.
- [46] N. M. O'Boyle, A. L. Tenderholt, K. M. Langner, *J. Comput. Chem.* **2008**, *29*, 839-845.
-

Entry for the Table of Contents (Please choose one layout)

Layout 1:

FULL PAPER

The study of up to sixteen corrole free bases bearing 5,15 *meso* ester groups show that these substituents have a strong electron withdrawing character while keeping the fluorescence of the parent macrocycle. Their low steric hindrance is illustrated in five crystal packings featuring short intermolecular distances between corroles that are stacked into columns.



*Gabriel Canard**, *Di Gao*, *Anthony D'Aléo*, *Michel Giorgi*, *Florian-Xuan Dang*, *Teodor Silviu Balaban**

Page No. – Page No.

Meso-Ester Corroles

Layout 2:

FULL PAPER

((Insert TOC Graphic here))

*Author(s), Corresponding Author(s)**

Page No. – Page No.

Title

Text for Table of Contents